

Anomalous decouplings and the fermion sign problem

Ghassan George Batrouni

Lawrence Livermore National Laboratory, P.O. Box 808, Livermore, California 94550

Richard T. Scalettar

Physics Department, University of California, Davis, Davis, California 95616

(Received 26 February 1990)

In expressing the partition function for a system of interacting electrons as a path integral, the effective Boltzmann weight is not sign definite. This limits our ability to reach very low temperatures in numerical simulations. While magnetic phase transitions are well studied, superconducting instabilities are much more elusive. In this paper we study the properties of the sign in a novel formulation of the path integral within the finite-temperature grand-canonical "determinantal" Monte Carlo method. The approach decouples the interaction into pair creation and annihilation operators rather than the particle number density operators previously used. We find that the average sign depends on the particular path-integral formulation and hence does not correspond to any physical observable. The asymptotic exponential behavior of $\langle s \rangle$ with β previously reported holds here as well but with a different decay constant.

I. INTRODUCTION

There are a number of alternate approaches to the study of systems of correlated electrons, from mean-field treatments and variational wave-function calculations to selective diagrammatic summations. One of the advantages of quantum Monte Carlo simulations is that, in principle, it treats the interactions in an exact way. However, these simulations have a number of limitations. The most severe is the fermion sign problem, which makes it difficult to reach low temperature.¹⁻⁴ This problem appears when the partition function is written as a path integral with the inverse temperature acting as imaginary time. The integrand, which is a product of determinants arising from tracing out the fermion operators, is not sign definite and therefore cannot be used directly as a probability density. The average sign decreases exponentially with β , which means that measurements of observables are obtained from cancellations of large numbers. This introduces large fluctuations in the results. In this paper we will study the behavior of the sign problem in detail for a new type of Hubbard-Stratonovich (HS) transformation in this determinant algorithm. So far, the sign problem has been studied only for a transformation that decouples the quartic Hubbard interaction into density operators. It is therefore unknown whether the sign problem, in this algorithm, is of physical significance or if it is an artifact of the way the partition function was formulated through the Trotter-Suzuki approximation and the particular HS transformation employed. The general belief is that the cause of the problem is the antisymmetry of fermion wave functions even in the determinant algorithm where no wave functions are used. Our results show that the sign problem does depend on the transformation, whereas the physical observables do not. This emphasizes that in the determinant algorithm, the aver-

age sign does *not* correspond to a physical observable.

The paper is organized as follows. In Sec. II we derive the path integral for the partition function and the decoupling of the Hubbard interaction both for the conventional and the new anomalous HS transformations. We also discuss some of the new features exhibited by the anomalous transformation. In Sec. III we discuss exact and simulation results for the Hubbard model in the non-hopping limit ($t=0$) in the anomalous decoupling scheme. Section IV deals with the Monte Carlo results for $t=1$ on 2×2 and 4×4 lattices, and Sec. V has conclusions and further discussions

II. PATH-INTEGRAL FORMULATION

A. Conventional Hubbard-Stratonovich transformation

We start this section by reviewing the path-integral formulation of the partition function for the Hubbard model via the Trotter approximation and the conventional HS transformation. The partition function in the grand-canonical ensemble is given by

$$Z = \text{tr}(e^{-\beta H}), \quad (2.1a)$$

$$H = -t \sum_{\langle ij \rangle, \sigma} [c_{\sigma}^{\dagger}(i)c_{\sigma}(j) + c_{\sigma}^{\dagger}(j)c_{\sigma}(i)] \\ + U \sum_i [n_{+}(i) - \frac{1}{2}][n_{-}(i) - \frac{1}{2}] \\ - \mu \sum_i [n_{+}(i) + n_{-}(i)]. \quad (2.1b)$$

The sum $\langle ij \rangle$ is over all pairs of nearest-neighbor lattice sites, t is the hopping parameter, $c_{\sigma}^{\dagger}(i)$ and $c_{\sigma}(i)$ are creation and annihilation operators for electrons of spin σ along the z axis at site i . U is the Coulomb coupling constant (in this paper we take it to be positive), β is the

inverse temperature, μ is the chemical potential and the number operator at site i is $n_\sigma(i) = c_\sigma^\dagger(i)c_\sigma(i)$.

For the purpose of performing numerical simulations, we need to represent the partition function as a path integral over classical fields.⁵ This proceeds via the Trotter-Suzuki approximation.⁶ The inverse temperature, β , is treated as imaginary time and is divided into L time intervals separated by $\tau = \beta/L$. We can therefore write

$$\begin{aligned} Z &= \text{tr}(e^{-\tau LH}) \\ &= \text{tr}(e^{-\tau(K+V)})^L \\ &\approx \text{tr}(e^{-\tau V} e^{-\tau K})^L, \end{aligned} \quad (2.2)$$

where

$$\begin{aligned} K &= -t \sum_{\langle ij \rangle, \sigma} [c_\sigma^\dagger(i)c_\sigma(j) + c_\sigma^\dagger(j)c_\sigma(i)] \\ &\quad - \mu \sum_i [n_+(i) + n_-(i)] \\ &= \sum_{\langle ij \rangle, \sigma} c_\sigma^\dagger(i)k_{ij}c_\sigma(j), \end{aligned} \quad (2.3)$$

and

$$V = U \sum_i [n_+(i) - \frac{1}{2}][n_-(i) - \frac{1}{2}]. \quad (2.4)$$

This Trotter-Suzuki approximation introduces errors of order τ^2 in physical observables because we ignored commutator terms between the kinetic and potential energies.⁷ The quartic interaction terms can be put into quadratic form at the expense of introducing a classical auxiliary field. This Hubbard-Stratonovich transformation can be done with continuous or discrete fields. In the discrete case (introduced by Hirsch⁴) we get

$$\begin{aligned} &\exp\{-\tau U [n_+(i) - \frac{1}{2}][n_-(i) - \frac{1}{2}]\} \\ &= \frac{e^{-\tau U/4}}{2} \sum_{s(i,l)=\pm 1} \exp\{-\lambda s(i,l)[n_+(i) - n_-(i)]\} \end{aligned} \quad (2.5)$$

at each site i and time slice l . λ is related to the Coulomb coupling constant by the relation

$$\cosh(\lambda) = e^{\tau U/2}. \quad (2.6)$$

Substituting Eqs. (2.3)–(2.5) in Eq. (2.2) we see that all operators in the partition function appear quadratically (repeated indices are summed and V is the spatial volume),

$$Z = \frac{e^{-\beta V U/4}}{2^{VL}} \sum_{\{s\}} \text{tr} \left[\prod_{l=1}^L \left\{ \exp\{-\tau [c_+^\dagger(i)k_{ij}c_+(j) + c_-^\dagger(i)k_{ij}c_-(j)]\} \exp\{-\lambda s(i,l)[n_+(i) - n_-(i)]\} \right\} \right], \quad (2.7)$$

and the trace can be easily done yielding the classical partition function (dropping the constant prefactor)

$$Z = \sum_{s(i,l)=\pm 1} \det M^+ \det M^-, \quad (2.8)$$

where

$$M^\sigma = I + B_L^\sigma B_{L-1}^\sigma \cdots B_1^\sigma \quad (2.9)$$

and

$$B_l^\pm = e^{\mp \lambda v(l)} e^{-\tau k}. \quad (2.10)$$

I is a $V \times V$ unit matrix (V is the spatial volume), and $v(l)_{ij} = \delta_{ij} s(i,l)$, where i runs from 1 to V , and l from 1 to L . Physical observables can be expressed⁵ in terms of the electron Green function, $(M^\sigma)^{-1}$, and to measure them we perform a classical Monte Carlo simulation in the auxiliary fields $s(i,l)$.

Before proceeding to the anomalous decoupling we wish to express Eq. (2.8) in a form that is more convenient for later comparisons. In Eq. (2.7) make the particle-hole variable change

$$d(i) = c_-^\dagger(i), \quad (2.11)$$

and for simplicity of notation drop the $+$ subscript on the c operators. Defining $n_c(i) = c^\dagger(i)c(i)$ and $n_d(i) = d^\dagger(i)d(i)$ gives

$$Z = \frac{e^{\beta V(\mu - U/4)}}{2^{VL}} \sum_{\{s\}} \text{tr} \left[\prod_{l=1}^L \left\{ \exp\{-\tau [c^\dagger(i)k_{ij}c(j) - d^\dagger(i)k_{ij}d(j)]\} \exp\{-\lambda s(i,l)[n_c(i) + n_d(i)]\} \right\} \right], \quad (2.12)$$

which can be written as

$$Z = \frac{e^{\beta V(\mu - U/4)}}{2^{VL}} \sum_{\{s\}} \text{tr} \left[\prod_{l=1}^L \left\{ \exp \left[-\tau (c^\dagger \ d^\dagger) \begin{pmatrix} k & 0 \\ 0 & -k \end{pmatrix} \begin{pmatrix} c \\ d \end{pmatrix} \right] \exp \left[-\lambda (c^\dagger \ d^\dagger) \begin{pmatrix} v(l) & 0 \\ 0 & v(l) \end{pmatrix} \begin{pmatrix} c \\ d \end{pmatrix} \right] \right\} \right]. \quad (2.13)$$

Doing the trace finally yields

$$Z = \frac{e^{\beta V(\mu - U/4)}}{2^{VL}} \sum_{\{s\}} \det \left[I + \prod_{l=1}^L C_l \right], \quad (2.14a)$$

where

$$C_l = e^{-\tau \sigma_z \otimes k} e^{-\lambda I \otimes v(l)} \quad (2.14b)$$

and

$$\sigma_z \otimes k = \begin{bmatrix} k & 0 \\ 0 & -k \end{bmatrix}. \quad (2.14c)$$

σ_z is the third Pauli matrix, I is the 2×2 identity matrix, and $v(l)$ is the $V \times V$ auxiliary field matrix defined in Eq. (2.10). This form of the partition function is completely equivalent to Eqs. (2.8)–(2.10) in the strong sense that the summands in both expressions are equal configuration by configuration.

B. Anomalous Hubbard-Stratonovich transformation

The preceding HS transformation is not unique. In particular, instead of transforming the quartic interaction term by introducing auxiliary fields coupled to the number density operators, we can introduce auxiliary fields coupled to pair creation and annihilation operators. Consider the operator Γ defined by

$$\Gamma(i) = c_+^\dagger(i) c_-^\dagger(i) + c_+(i) c_-(i). \quad (2.15)$$

Then we can prove the operator identity

$$\begin{aligned} \exp\{-\tau U [n_+(i) - \tfrac{1}{2}][n_-(i) - \tfrac{1}{2}]\} \\ = \frac{e^{\tau U/4}}{\sqrt{2\pi}} \int_{-\infty}^{+\infty} dx e^{-x^2/2 + \sqrt{\tau U} x \Gamma(i)} \end{aligned} \quad (2.16)$$

by first expanding $e^{\sqrt{\tau U} x \Gamma(i)}$ in a power series in $\Gamma(i)$, then using the identities

$$\Gamma^2(i) = -2[n_+(i) - \tfrac{1}{2}][n_-(i) - \tfrac{1}{2}] - \tfrac{1}{2} \quad (2.17a)$$

and

$$\Gamma^4(i) = -\Gamma^2(i) \quad (2.17b)$$

to do the integrals term by term and resum the series. The identity Eq. (2.16) can be used to perform a Hubbard-Stratonovich transformation, with continuous auxiliary fields, thus enabling us to do the trace over the fermion operators since they now appear only quadratically. We will, however, concentrate on the corresponding discrete transformation as we did in subsection A.

It is perhaps a bit surprising that there is a discrete form of the transformation defined in Eq. (2.16). This is

$$\begin{aligned} \exp\{-\tau U [n_+(i) - \tfrac{1}{2}][n_-(i) - \tfrac{1}{2}]\} \\ = \frac{e^{\tau U/4}}{2} \sum_{s(i,l)=\pm 1} e^{\gamma \Gamma(i)s(i,l)}, \end{aligned} \quad (2.18a)$$

where γ is defined by

$$\cos(\gamma) = e^{-\tau U/2} \quad (2.18b)$$

and $\Gamma(i)$ is defined in Eq. (2.15). It is interesting to compare our new discrete transformation with that previously defined by Eqs. (2.5) and (2.6). One marked difference is the limit of the two coupling parameters λ and γ as the Coulomb coupling constant U gets very large. As $U \rightarrow \infty$ so does λ , whereas $\gamma \rightarrow \pi/2$. The significance of this will be further elaborated in the following.

We now use this discrete transformation to implement a HS transformation. Substitute Eqs. (2.3), (2.4), and (2.18a) in the Trotter-Suzuki formula Eq. (2.2) to obtain

$$Z = \frac{e^{\beta V U/4}}{2^L} \sum_{\{s\}} \text{tr} \left[\prod_{l=1}^L \left[\exp\{-\tau [c_+^\dagger(i) k_{ij} c_+(j) + c_-^\dagger(i) k_{ij} c_-(j)]\} e^{\gamma s(i,l) \Gamma(i)} \right] \right], \quad (2.19)$$

where repeated indices are summed. Again the fermionic operators appear quadratically and the trace can be done. To perform the trace we make the particle-hole variable change, Eq. (2.11), and proceed in the same manner as with Eqs. (2.12) and (2.13). This finally gives the classical partition function

$$Z = \frac{e^{\beta V(\mu + U/4)}}{2^{LV}} \sum_{\{s\}} \det \left[I + \prod_{l=1}^L D_l \right], \quad (2.20a)$$

where

$$D_l = e^{-\tau \sigma_z \otimes k} e^{i \gamma \sigma_y \otimes v(l)} \quad (2.20b)$$

and

$$\sigma_y \otimes v(l) = i \begin{bmatrix} 0 & -v(l) \\ v(l) & 0 \end{bmatrix}. \quad (2.20c)$$

σ_y is the second Pauli matrix. For completeness, we

point out that instead of using $\Gamma(i)$ [see Eq. (2.15)] in our anomalous decoupling scheme, we could have used

$$\Gamma'(i) = c_+^\dagger(i) c_-^\dagger(i) - c_+(i) c_-(i), \quad (2.21)$$

which gives the partition function

$$Z = \frac{e^{\beta V(\mu + U/4)}}{2^{LV}} \sum_{\{s\}} \det \left[I + \prod_{l=1}^L F_l \right], \quad (2.22a)$$

where

$$F_l = e^{-\tau \sigma_z \otimes k} e^{i \gamma \sigma_x \otimes v(l)} \quad (2.22b)$$

and

$$\sigma_x \otimes v(l) = \begin{bmatrix} 0 & v(l) \\ v(l) & 0 \end{bmatrix}. \quad (2.22c)$$

σ_x is the first Pauli matrix. Note that whereas the matrices D_l are real, F_l are complex.

C. Discussion

The problem of evaluating the expectation value of physical observables has been reduced to that of performing Monte Carlo simulations on one of the equivalent systems given by Eq. (2.14), Eqs. (2.20), or Eqs. (2.22). An efficient algorithm to simulate system (2.14) was first developed in Ref. 4 and extended to low temperatures in Ref. 3. It is equally applicable to (2.20). This algorithm may need some modification to study system (2.22) because this system has complex matrices, while the algorithm was developed for real matrices. Here we concentrate on (2.20).

The major problem encountered in simulations with the conventional decoupling [Eqs. (2.14a)–(2.14c)] is that the configuration sum in Eq. (2.8) or (2.14a) cannot always be easily done by Monte Carlo methods because the summand can have different signs for different configurations of the auxiliary field $\{s\}$. This means that the summand cannot be used as a probability density in numerical simulations. In practice what has been done is to consider the absolute value of the summand as a probability density and explicitly keep track of the changing sign. For details, see Refs. 1–4. This has small fluctuations when the average of the determinants

$$\langle s \rangle = \frac{\sum_{\{s\}} \det M}{\sum_{\{s\}} |\det M|}, \quad (2.23)$$

is not far from unity. For values that are much smaller than one the method becomes less practical, and in the physically interesting region of the positive U Hubbard model, i.e., large β and doped away from half filling, the problem is most severe. It was shown numerically that the average sign tends to zero exponentially:

$$\langle s \rangle \sim e^{-\beta c}, \quad (2.24)$$

where c is a constant. Clearly this makes simulations at low temperatures very hard to do. Meanwhile, ignoring the sign completely can give reasonable values for some observables, but gets even the qualitative behavior of others completely wrong.¹

It was noticed^{1,8} that at least some of the auxiliary-field configurations that lead to negative determinants correspond to a pair of electrons or holes whose paths cross as the pair evolves from imaginary time $t=0$ to imaginary time $t=\beta$. This is because the auxiliary field is coupled to the number density operator (actually to the magnetization) and therefore acts as a chemical potential which locally enhances or suppresses the density of particles. If the probability of these path crossings in a given imaginary time interval $\Delta\beta$ approaches a constant at low temperature, then the exponential decay law follows directly from phase-space considerations. This provided a convenient qualitative picture of the origin of the sign problem valid within the normal decoupling.

Before moving on to numerical results we wish to make some observations about the form of the three decoupling schemes we presented here. Comparing Eqs. (2.14), (2.20), and (2.22) we see that they all have the same gen-

eral form, namely that of a sum over configurations of the auxiliary field, which appears in a determinant. Also the kinetic-energy part in all schemes appears as $e^{-\tau\sigma_z \otimes k}$. As for the auxiliary-field parts, different matrices (I , σ_x , and σ_y) multiply the auxiliary-field matrix. We have not found an anomalous transformation that introduces a σ_z into the auxiliary-field part of the determinant. There is such a transformation for the normal decoupling, and it leads to Eqs. (2.14) but with $e^{-\lambda I \otimes v(l)}$ replaced by $e^{-i\lambda\sigma_z \otimes v(l)}$. It is interesting that the four preceding decouplings are related by the generators of the $U(2)$ group. Note that although the partition functions in all decoupling schemes are equal, the determinants are not equal configuration by configuration for the normal and anomalous decoupling schemes. It is this that raises the possibility that the sign problem could be a function of the HS transformation.⁹

III. NUMERICAL SIMULATIONS: $t=0$

We want to study the behavior of the $\langle s \rangle$ in the anomalous decoupling scheme. The no-hopping limit of the Hubbard model is well suited for that for two reasons. First, we know the exact solution so we can easily check numerical results, and second there are no finite time step, τ , errors due to the Trotter-Suzuki approximation. This will allow us to study the algorithm for various time step sizes without worrying about the errors introduced into the observables. Also, recall that in the normal decoupling scheme there is *no* sign problem at all in the no-hopping limit ($t=0$). The reason is that for $t=0$ all the B_l^σ matrices in Eqs. (2.8)–(2.10) commute and are diagonal, so it is easy to prove that all the eigenvalues of M^σ are positive for any auxiliary-field configuration. This is not true for anomalous decoupling, and therefore even in the $t=0$ limit the sign problem still exists. This offers a very simple model to study this complicated phenomenon.

We want to study the system given by Eqs. (2.20). With $t=0$ it collapses to independent one-site systems, and by Eqs. (2.3) and (2.20) we get

$$\prod_{l=0}^L D_l = \prod_{l=1}^L e^{\tau\mu\sigma_z} e^{i\gamma\sigma_y v(l)}. \quad (3.1)$$

We can easily evaluate exactly the partition function, the average sign, and physical observables for $L \leq 20$ by sorting through all configurations of the auxiliary field. For $L > 20$ this becomes too time consuming and these quantities are evaluated by Monte Carlo to very high accuracy. We also made sure that physical observables ($\langle n \rangle$ and $\langle n_+ n_- \rangle$) from our algorithm always agreed with exact results.

Figure 1 is a plot of $\log_{10}(\langle s \rangle)$ versus β and shows the familiar exponential decay of the sign as the temperature decreases. We also made the same plot but for $U=30$ and $\langle n \rangle=0.4$ and again found exponential decay. It is very interesting that the same exponential behavior, which is observed in the normal decoupling scheme (with $t \neq 0$) and attributed to crossing fermion paths, is also observed in the one-site problem where no such paths exist.

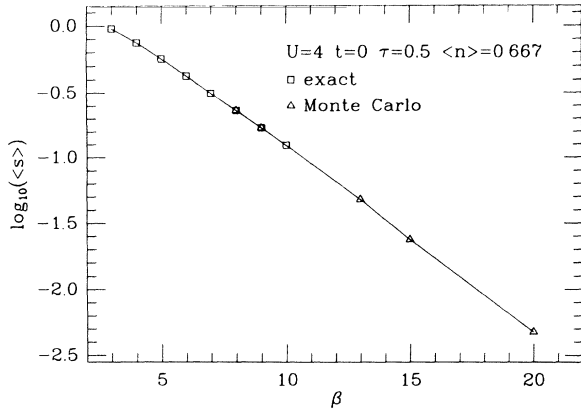


FIG. 1. $\log_{10}(\langle s \rangle)$ vs β for the Hubbard model in the no-hopping limit. The errors for the Monte Carlo are smaller than the point sizes.

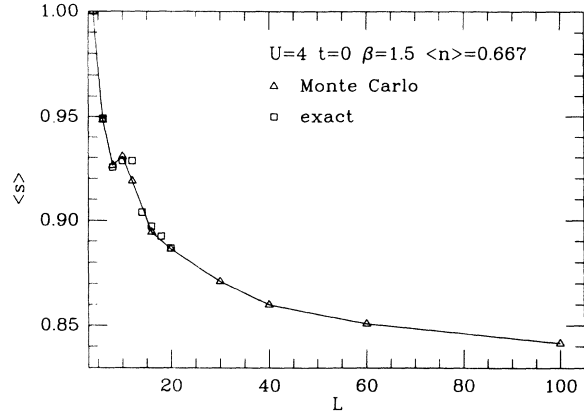


FIG. 3. $\langle s \rangle$ vs the number of time slices, L , at fixed β . The average sign appears to approach limiting value as $L \rightarrow \infty$, i.e., as $\tau = (\beta/L) \rightarrow 0$.

Furthermore, a plot of $\langle s \rangle$ versus occupation ($\langle n \rangle$), Fig. 2, again shows the same qualitative features observed with conventional decoupling. The plots for two-dimensional lattices show more structure due to the band effects, which are of course absent in the one site problem. This very close similarity between Figs. 1 and 2 for the one-site problem and the corresponding plots for two-dimensional lattices with conventional decoupling³ leads us to believe that similar mechanisms are at play in both cases. In Fig. 3 we show the behavior of $\langle s \rangle$ versus the number of time slices L or equivalently the time step τ at constant β . We see that there is a relatively mild dependence of $\langle s \rangle$ on the size of the time step. As the number of time slices increases $\langle s \rangle$ decreases, but this decrease is not exponential. It appears that for the physical parameters shown in Fig. 3, $\langle s \rangle$ reaches a limiting value of about 0.84 as $L \rightarrow \infty$, i.e., as $\tau \rightarrow 0$. We also checked this for $\beta=6$ and $\langle n \rangle=0.4$ and observed the same effect. Again this behavior agrees well with conventional decoupling results for $t \neq 0$ where $\langle s \rangle$ is found to have little dependence on τ . Note, however, that when

$t \neq 0$ one cannot make L arbitrarily small because that makes the time step τ large and introduces finite time step errors which are unacceptably large. Thus the conventional wisdom that $\langle s \rangle$ depends on β and not on τ or L is to be understood to assume that τ is small enough to give good results for observables. If it were possible to increase τ to larger values, $\langle s \rangle$ would be considerably better behaved. When $t=0$ there are no finite time step errors which enables us to make τ as large as β . It is interesting to note that in this limit physical quantities like the occupation and energy have *no* τ (or equivalently L) dependence whereas $\langle s \rangle$ *does*.

Next we checked our observation in Sec. II that since for large U that anomalous coupling constant saturates at $\gamma = \pi/2$, it may also lead to the saturation of $\langle s \rangle$. Figure 4 shows a plot of $\langle s \rangle$ versus U for two different temperatures. We see that indeed the average sign does saturate, for $U \approx 10$ ($\tau U \approx 5$), at a value which seems to depend on the temperature. The large value of τU is not troublesome here because there are no finite time step errors in the one-site model. This however, is not so for Monte

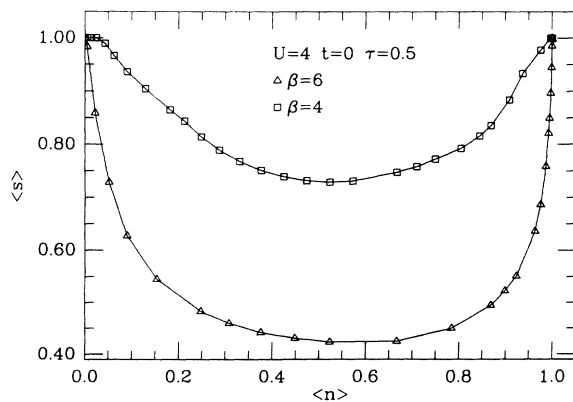


FIG. 2. Dependence of average sign on the average occupation in the no-hopping limit. All the points were obtained by exact evaluations, there are no error bars.

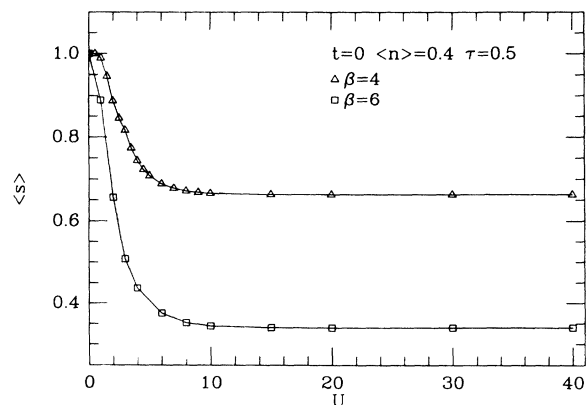


FIG. 4. This plot shows how the values of the average sign saturates for large U .

Carlo simulations with the nonzero hopping parameter, t , where in the simplest Trotter-Suzuki breakup the errors are of order $\tau^2 t U$. Then as U increases τ must decrease with $\tau^2 t U$ constant in order to keep the systematic errors fixed. This means that τU is still increasing and that eventually, by Eq. (2.18b), γ will saturate, and so will $\langle s \rangle$. This could be useful for simulation at very large U , especially if a higher-order breakup is used¹⁰ which allows larger τ .

We also checked the behavior of Eq. (2.22) where, since the matrices F_l are complex, it might appear that the determinant will also be complex. We found that the determinants are always real, and that they are equal configuration by configuration to those from Eq. (2.20). So, both anomalous decoupling schemes, Eq. (2.20) and (2.22), behave identically.

To summarize, we have found that $\langle s \rangle$ for the *single-site* Hubbard model ($t=0$) in the anomalous decoupling scheme exhibits qualitatively the same behavior previously observed for the $t \neq 0$ case with conventional decoupling. A similar sign problem in small size systems was observed in simulations of the Anderson lattice in the limit where the conduction p orbital overlap is zero but the hybridization to the local d orbital is not.¹¹

IV. NUMERICAL SIMULATIONS: $t \neq 0$

In this section we study the systematics of the sign problem when the hopping parameter, t , is not zero. We start by examining the effect of the finite time step, τ , on physical observables. Figure 5 shows a plot of the kinetic energy versus the time step τ for anomalous and normal decoupling. We see that the systematic errors in both cases are the same, and that the kinetic energy converges to the same value as $\tau \rightarrow 0$. The horizontal line is the value obtained from exact diagonalization. Figures 6 and 7 show the same behavior for the potential energy and antiferromagnetic structure function, respectively. This shows that we have control over the systematic errors and that the algorithm works properly.

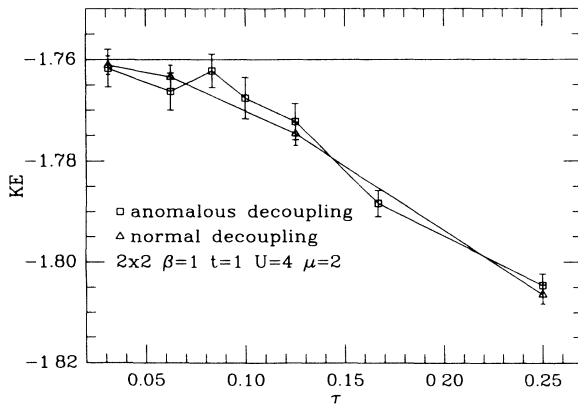


FIG. 5. A plot of the kinetic energy vs τ for the Hubbard model on a 2×2 lattice, for both normal and anomalous decoupling. It shows the anomalous decoupling results agreeing with normal decoupling. The horizontal line is from exact diagonalization.

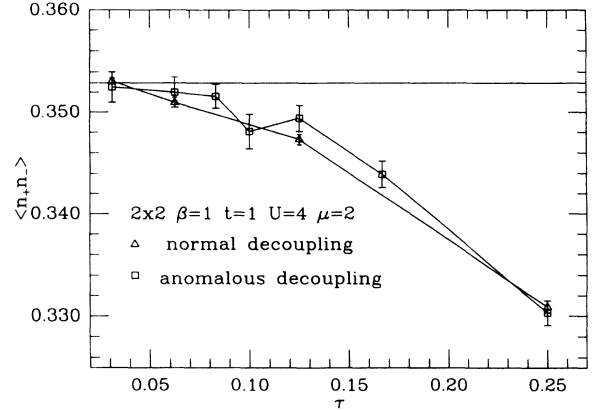


FIG. 6. The same as Fig. 5 but for $n_+ n_-$ vs τ . The horizontal line is from exact diagonalization.

Figure 8 shows a plot of $\langle s \rangle$ versus the average occupation, $\langle n \rangle$. It exhibits the same qualitative behavior observed for normal decoupling in Fig. 10(a) of Ref. 3, including the appearance of a peak at $\langle n \rangle \approx 0.6$. Notice, however, that whereas the peak in the normal decoupling is pinned at $\langle s \rangle = 1$ (for the particular set of parameters used) its height varies with β in the anomalous decoupling. This says that the band effects are qualitatively the same and influence the average sign in the same way but to different degrees. Also notice in Fig. 8 that at zero chemical potential (i.e., at half filling), $\langle s \rangle = 1$ just as for normal decoupling. Another curious effect we noticed is that at zero chemical potential $\langle n_+ \rangle = \langle n_- \rangle = 0.5$ exactly with no statistical fluctuations. We believe this is due to the fact that the auxiliary field does not couple to a number operator, and therefore does not act as a fluctuating chemical potential.

Finally, Fig. 9 shows the average sign versus β , and exhibits the familiar exponential decay. The slope is approximately -1.07 , whereas the corresponding slope for the normal decoupling, from Fig. 5 of Ref. 1, is -0.7 .

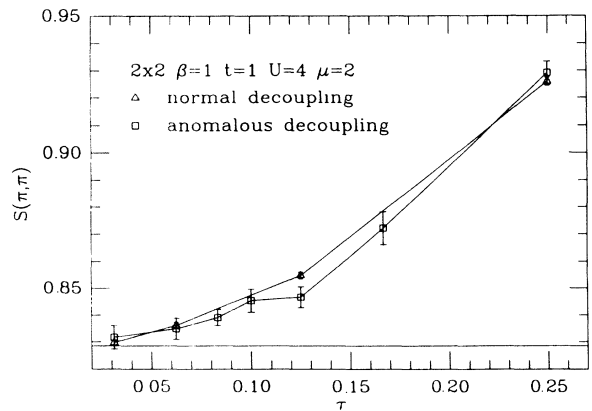


FIG. 7. The same as Fig. 5 but for the antiferromagnetic structure function, $S(\pi, \pi)$ vs τ . The horizontal line is from exact diagonalization.

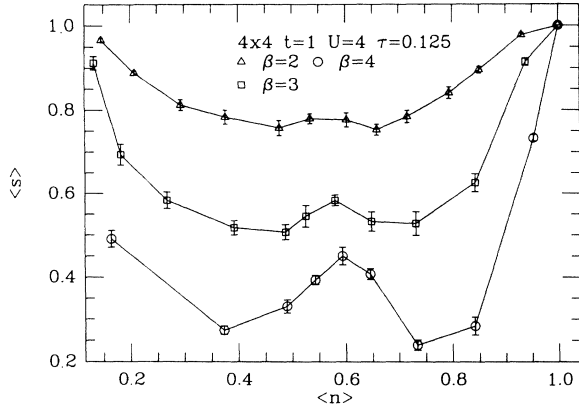


FIG. 8. This plot shows the dependence of $\langle s \rangle$ on the occupation for anomalous decoupling and exhibits the same peak and general structure seen for normal decoupling.

Note that these slopes are calculated using the natural logarithm, while our Fig. 9 shows \log_{10} . The data in Ref. 1 is for the canonical rather than the grand-canonical ensemble, but their Fig. 6 shows data for both ensembles and the slopes are equal and this is what we will assume. Therefore, since the slope depends on the transformation, it does not correspond to a physical observable.

V. CONCLUSIONS

Using the normal Hubbard-Stratonovich transformation in the determinant algorithm, it was noticed that certain configurations of the auxiliary field lead to negative determinants. It was then suggested^{1,8} that this sign problem is caused by the crossing of fermion paths because the auxiliary field couples to the number operator and acts as a chemical potential which guides the paths of the fermions. This prompted us to derive anomalous Hubbard-Stratonovich transformations where the auxiliary field does not couple to single-particle number operators but instead couples to creation and annihilation

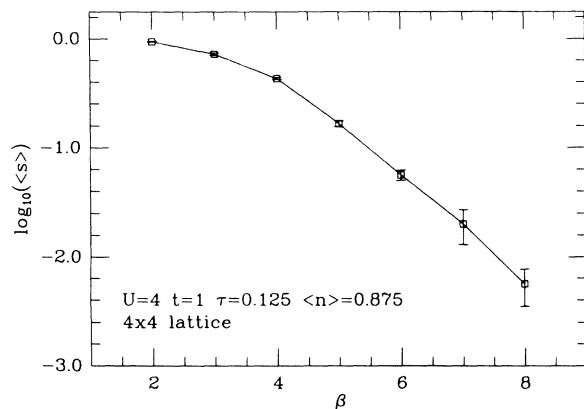


FIG. 9. $\log_{10}(\langle s \rangle)$ vs β for anomalous decoupling on 4×4 lattice. It shows the by now typical exponential decay of the average sign as β increases.

operators of fermion *pairs*. The auxiliary field then couples to effective boson operators that might significantly modify the sign problem. We found that the sign problem is still present for the anomalous decoupling even in the no-hopping limit, $t=0$, where normal decoupling determinants are positive definite. We also found that although for $t=0$ *physical* observables do not depend on the time step, the average sign does. Furthermore, we found that while the properties of $\langle s \rangle$ are *qualitatively* the same in the normal and anomalous decoupling schemes the slope of the exponential decay is not universal. Therefore, the sign problem and the “world line” interpretation are not intrinsic properties of the model Hamiltonian, but depend on the decoupling scheme employed in the determinant algorithm.

The world line picture of the origin of the sign problem within the usual density decoupling has another interesting feature: A configuration of Hubbard-Stratonovich fields which forces the exchange of two up-spin electrons, and hence has an up-spin determinant which is negative, will also represent the exchange of two down-spin holes. The down-spin determinant will therefore also be negative, and the product of the two determinants will tend to be positive. Thus, while the world line picture provides a feeling for the sorts of configurations that might result in negative individual determinants, there is a somewhat less complete understanding of those that lead to a negative product.

The dependence of the average sign on the decoupling is not too surprising in view of the definition of the average sign,

$$\langle s \rangle = \frac{Z}{\tilde{Z}}. \quad (5.1)$$

Z is the partition function and \tilde{Z} is the partition function using the absolute value of the determinant as a weight. Z is independent of the decoupling scheme, while \tilde{Z} is *not*. As a consequence, it is clear that $\langle s \rangle$ must depend on the details of the path-integral formulation. This is consistent with the fact that similar “sign problems” in quantum spin simulations can be altogether eliminated by simple sublattice spin rotations.

A common feature of $\langle s \rangle$ in the anomalous and normal decoupling schemes is its exponential decay, $\langle s \rangle \approx e^{-\beta c}$. The origin of this in both decoupling schemes can be understood as follows. There are certain configurations of the auxiliary fields that lead to negative determinants. These configurations do not correspond to, and cannot be characterized by, physical observables because of the quantitative differences in $\langle s \rangle$ depending on the decoupling scheme. Regardless of the particular characterization of these configurations, when there is a large enough number of time slices and a finite, *temperature-independent* correlation length in the time direction, there will be domains of these imaginary time intervals with independent probabilities of having one of these configurations. The independence of these probabilities leads to the exponential decay law¹² in both decoupling schemes. To test this idea, we measured the correlation length in the time direction as a function of temperature for the $t=0$ case. We found for the parame-

ters of Fig. 1 that the correlation length indeed reaches the constant value of ≈ 0.5 for $\beta \geq 3$. For $U=4$, $\tau=0.5$, and $\langle n \rangle = 0.875$, the correlation length becomes constant (≈ 0.54) for $\beta \geq 5$. It follows that for a given value of β , the decoupling scheme that has the longest such domains, i.e., the most correlations in the imaginary time direction, will have the mildest sign problem.

This picture is further supported by the fact that in models where the fields which couple to the electronic degrees of freedom have intrinsic dynamics in the imaginary time direction, such as electron-phonon Hamiltonians, the sign changes of a single-spin determinant are significantly moderated.

One of the new features of the anomalous decoupling is that the coupling constant γ [see Eq. (2.18b)] saturates for large τU . This raises the possibility of simulations at large U , whereas τU is large while the systematic error $\sim \tau^2 t U$ is still small. This may be easier to achieve in a higher-order Trotter-Suzuki breakup than the one used here.

Finally, the discussion so far has been for positive U . When H is negative, all the transformations go through in exactly the same way, except that $\gamma \rightarrow i\gamma$ in Eq. (2.18b). This makes the matrices in Eqs. (2.20) complex and (2.22) real. However, we found that for $t=0$ the determinants in both cases are always real, *positive*, and equal configuration by configuration. Of course for $U < 0$ and normal decoupling the determinants are also always positive in the absence of an external magnetic field, but

not equal configuration by configuration to the anomalous case. We believe the same is true for $t \neq 0$. This means that for $U < 0$ the sign problem is absent in the anomalous decoupling scheme as it is in normal decoupling. It is easy to prove this for the normal case where we can show that $\det M^+ = \det M^-$ in Eq. (2.8), but no such thing happens with anomalous decoupling. It is interesting that, in the anomalous decoupling, the only difference between positive and negative U is that in the latter case the matrices D_l in Eq. (2.20) become complex ($i\sigma_y \rightarrow \sigma_y$) and that this single change makes the determinants always positive.

The normal density decoupling is also the one used in zero-temperature canonical simulation studies,^{1,2,11} where a sign problem is again encountered. However, there is an additional freedom in choosing the trial wave function from which the projection begins and which affects the average sign. It would be interesting to study the sign properties of this ground-state algorithm with our new decoupling. In particular some BCS-type trial wave function might have interesting properties.

ACKNOWLEDGMENTS

We thank B. Alder, K. Dawson, E. Loh, R. Sugar, and S. White for fruitful discussion. G.G.B.'s work was performed under the auspices of the U.S. Department of Energy by the Lawrence Livermore National Laboratory under Contract No. W-7405-ENG-48.

¹E. Y. Loh, Jr., J. E. Gubernatis, R. T. Scalettar, S. R. White, D. J. Scalapino, and R. L. Sugar, Phys. Rev. B **41**, 9301 (1990).

²S. Sorella, S. Baroni, R. Car, and M. Parinello, Europhys. Lett. **8**, 663 (1989); S. Sorella, E. Tosatti, S. Baroni, R. Car, and M. Parinello, Int. J. Mod. Phys. B **1**, 993 (1988).

³S. R. White, D. J. Scalapino, R. L. Sugar, E. Y. Loh, J. E. Gubernatis, and R. T. Scalettar, Phys. Rev. B **40**, 506 (1989).

⁴J. E. Hirsch, Phys. Rev. B **31**, 4403 (1985).

⁵R. Blankenbecler, D. J. Scalapino, and R. L. Sugar, Phys. Rev. D **24**, 2278 (1981).

⁶H. F. Trotter, Proc. Am. Math. Soc. **10**, 545 (1959); M. Suzuki, Comm. Math. Phys. **51**, 183 (1976).

⁷R. M. Fye, Phys. Rev. B **33**, 6271 (1985); R. M. Fye and R. T. Scalettar, *ibid.* **36**, 3833 (1987).

⁸J. E. Hirsch (private communication).

⁹In fact, Hirsch [Phys. Rev. B **34**, 3216 (1986)] has introduced a transformation using two auxiliary fields which couple to the charge and spin and smoothly interpolates between the "determinantal" Monte Carlo technique described here and a second "world line" approach. He finds that the sign problem depends on the value of the interpolating parameter.

¹⁰S. Fahy and D. R. Hamann (unpublished).

¹¹R. M. Fye (private communication).

¹²This argument follows closely that in Ref. 1 except that we do not physically characterize the auxiliary-field configurations.